EFFECT OF SURFACTANTS ON LIQUID SIDE MASS TRANSFER COEFFICIENTS

Pisut Painmanakul[1], Karine Loubière[1], Gilles Hébrard[1],

Martine Mietton-Peuchot[2] and Michel Roustan[1]

[1] Laboratoire d'Ingénierie des Procédés de l'Environnement, Dpt G.P.I., Institut National des Sciences Appliquées, 135 avenue de Rangueil, 31077 Toulouse Cedex 4, FRANCE.

[2] Laboratoire de Génie des Procédés JE2241 Faculté d'œnologie Victor Ségalen Bordeaux 2 33405

Abstract

In the present paper, the effect of liquid properties (surfactants) on bubble generation phenomenon, interfacial area and liquid side mass transfer coefficient was investigated. The measurements of surface tension (static and dynamic methods), of Critical Micelle Concentration (CMC) and of characteristic adsorption parameters such as the surface coverage ratio at equilibrium (s_e) were performed to understand the effects of surfactants on the mass transfer efficiency. Tap water and aqueous solutions with surfactants (cationic and anionic) were used as liquid phases and an elastic membrane with a single orifice as gas sparger. The bubbles were generated into a small-scale bubble column. The local liquid side mass transfer coefficient (k_L) was obtained from the volumetric mass transfer coefficient (k_La) and the interfacial area (a) was deduced from the bubble diameter (D_B), the bubble frequency (f_B) and the terminal bubble rising velocity (U_B). Only the dynamic bubble regime was considered in this work (Re_{OR} = 150 - 1000 and We = 0.002 - 4).

This study has clearly shown that the presence of surfactants affects the bubble generation phenomenon and thus the interfacial area (a) and the different mass transfer parameters, such as the volumetric mass transfer coefficient (k_La) and the liquid-side mass transfer coefficient (k_L). Whatever the operating conditions, the new k_La determination method has provided good accuracy without assuming that the liquid phase is perfectly mixed as in the classical

method. The surface coverage ratio (s_e) proves to be crucial for predicting the changes of k_L in aqueous solutions with surfactants.

Keywords: Surfactants, Bubble diameter; Bubble formation frequency; Interfacial area; Volumetric mass transfer coefficient; Liquid-side mass transfer coefficient; Surface coverage ratio.

1. INTRODUCTION

In gas-liquid reactors, mass transfer from the gas phase to the liquid phase is a key parameter of the process. Classically, gas is released in the form of small bubbles to yield a large surface area and also an efficient mass transfer between gas and liquid phases. Depending on the industrial operating conditions, various gas spargers can be used as aeration systems (perforated plate, porous disk diffuser, membrane gas sparger). To improve the mass transfer efficiency, the interfacial area and the liquid side mass transfer coefficient have to be controlled closely. The objective of the present study is to evaluate the effect of surfactants on interfacial area and liquid side mass transfer coefficient. Only the dynamic bubble regime will be considered here (Re_{OR} = 150 - 1000 and We = 0.002 - 4).

Several studies about the bubble diameters (D_B) present in bubble columns and generated from different types of gas spargers have been recently published [1-5]; in particular, it is interesting to note that the interfacial area (a) can be experimentally determined by using detached bubble diameters (D_B), bubble formation frequencies (f_B) and terminal bubble rising velocities (U_B) as [5].

The effects on bubble generation of liquid phase properties, such as density and viscosity, have been widely evaluated [6] whereas little investigation has been carried out on the liquid surface tension. Loubière and Hébrard [7] have studied the influence of surfactants on the bubble formation at different gas spargers, especially on the generated bubble diameter (D_B),

the associated bubble frequency (f_B) and the interfacial area (a). In this study, the liquid phases were characterized in terms of static and dynamic surface tensions, Critical Micelle Concentration (CMC) and characteristic adsorption parameters (surface coverage ratio at equilibrium (s_e), adsorption constant at equilibrium (K) and surface concentration when it is saturated (Γ_∞)). These authors have observed that the effect of surface tension on the bubble generated depends on the type of orifice (flexible and rigid) and should be analyzed in terms of dynamic surface tension and of kinetics of surfactant molecule adsorption and diffusion.

The literature about mass transfer parameters shows that there is a very limited number of qualitative data related to the influence of surface tension on the volumetric mass transfer coefficient (k_La); moreover, the k_La values are often global and thus insufficient to understand the gas liquid mass transfer mechanisms [8-9]. In this purpose, it becomes essential to separate the parameters, especially the liquid-side mass transfer coefficient (k_L) and the interfacial area (a) [10-12]; however, there is a lack of studies dealing with this separation in the presence of surfactants [13-15].

To fill this gap**,** the general aim of this present study is to propose a local experimental approach which enables the mass transfer efficiency to be effectively controlled whatever the operating conditions. The scope of this work is as follows:

- Characterisation of several liquid phases in terms of static and dynamic measurements of surface tension, Critical Micelle Concentration (CMC) and their associated characteristic adsorption parameters;
- Application of the new experimental method to determine the local volumetric mass transfer coefficient, the local interfacial area and thus the local liquid-side mass transfer coefficient;

- Quantification of the effect of surfactants on the bubble generation phenomenon, the interfacial area and the associated local mass transfer parameters (k_La and k_L).

For this purpose, this paper will firstly present the material and the experimental methods used in this work. Then, the characterisation of liquid phases under test will be described as well as the local mass transfer parameter determination (interfacial area provided by a sparger, volumetric mass transfer coefficient obtained with the new method, liquid-side mass transfer coefficient). Finally, the influence of the surfactants on the bubble generation and on the different mass transfer parameters will be shown; a simple model for estimating k_L will be proposed and applied whatever the operating conditions.

2. MATERIAL AND METHODS

2.1 EXPERIMENTAL SET-UP

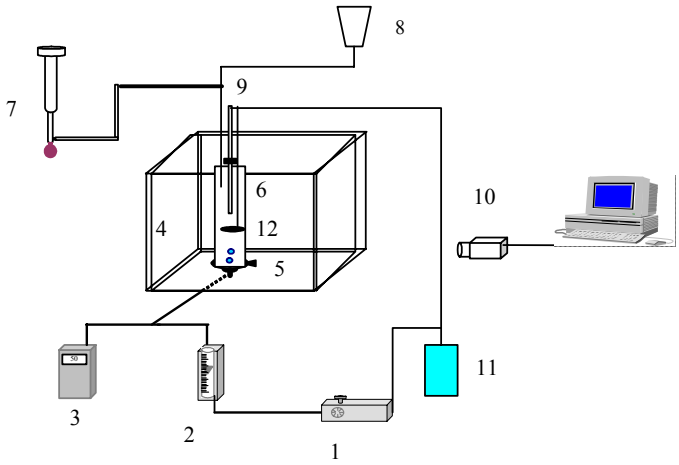

1 Pressure gauge
2 Gas flow meter
3 Electronic manometer
4 Bubble generation vessel
5 Membrane sparger
6 Bubble column
7 Soap film meter
8 Chemical solution
9 Oxygen microsensor
10 Acquisition computer & camera
11 Nitrogen pressure gauge
12 Agitation system

Figure 1. Schematic diagram of the experimental set-up

The experimental set-up is schematically represented in Figure 1. The experiments are carried out in a glass bubble column (6), 0.05 m in diameter, 0.40 m in height. This column is fixed

into a glass parallelepiped vessel (4), 0.40 m in width, 0.40 m in length, 0.30 m in height. The flow of air is monitored by a pressure gauge (1) and regulated by a gas flow meter (2). The pressure drop created by the membrane sparger is determined using an electronic manometer type BIOBLOCK 915PM247 (3). The average gas flow rate is measured using a soap film meter (7), through a funnel (1.5 cm diameter) put on the orifice. Nitrogen flow (employed for oxygen elimination in the liquid phase and for oxygen elimination at the top of the bubble column) is controlled by a pressure gauge (11). The UNISENSE oxygen microsensor, whose response time is very fast (as low as 50 ms), is used to measure the change in dissolved oxygen concentration (9). All chemical solutions (8) are injected at the top of the column. The operating conditions are as follows: liquid height H_L = 25 cm and temperature T = 20 ^{o}C.

In this work, pieces of 60 mm diameter of an industrial (Dégremont®) rubber membrane sparger are used as gas spargers. The bubbles are generated by a single puncture located at the membrane centre. As punctures were initially distributed over the entire surface sheet, it was necessary to close several holes without modifying the elastic membrane properties [16]. For this purpose, a silicone elastomer glue applied on the inner surface (gas chamber side) was used (Figure 2a).

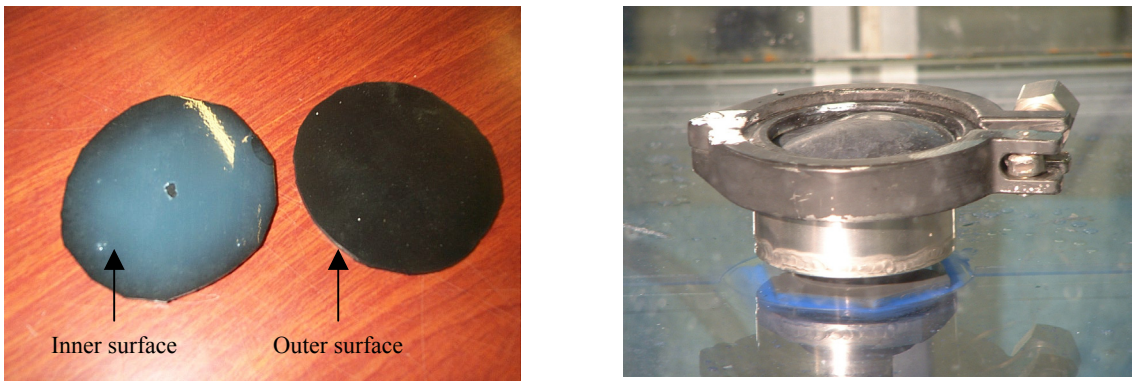

(a) (b)

Figure 2. (a) Inner and outer surfaces of an industrial membrane

(b) Membrane fixing system

The membrane is assembled on a circular clamping ring composed of two jaws (Figure 2b);

this fixing system coupled with the use of a dynamometric spanner enables the same initial tension to be applied, thus giving reproducible results. The physical characteristics of the membrane sparger and the operating conditions are reported in Table 1.

Table 1. Physical characteristics of the membrane sparger and operating conditions

Sparger	Thickness (mm)	Vc (cm^3)	γc (mN/m)	D_{OR} (mm)	Q_G (ml/s)
Membrane	2.06	33.4	23	0.29 – 0.40	0.3 – 3.5

2.2 IMAGE ACQUISITION AND TREATMENT METHOD

The bubble diameter generation is photographed with a Leutron LV95 camera (120 images/s). Images are visualised on the acquisition computer through the Leutron vision software. The image treatment is performed with the Visilog 5.4 software (C^{++} program).

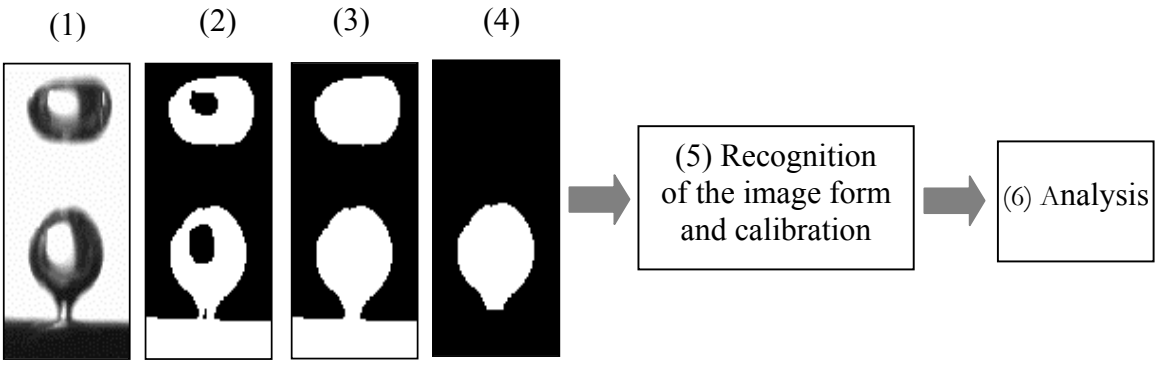

Figure 3 Typical sequence of image treatment: (1) Image acquisition (2) Image binarisation (3) Image completion (4) Border image delation

Figure 3 presents a typical sequence of image treatment. This treatment is based on a transformation of the acquired image into a binary image, followed by different arithmetical and geometrical operations. Then, the images are given uniform surface treatment (bubble

area A_B) and superfluous images are removed. The bubbles are spherical at low gas flow rates but become ellipsoidal at high gas flow rates. For ellipsoidal bubbles, the geometrical characteristics (length l, height h as shown in Figure 4b) are measured and an equivalent bubble diameter is calculated by the equation (2); for spherical bubbles, the equation (1) is considered to calculate the diameter (Figure 4a). From the measurement of 100-150 bubbles, an average bubble diameter is deduced.

(a) Spherical bubble

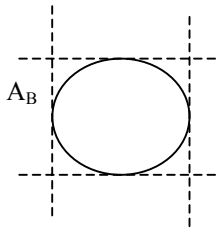

$$D_B = \sqrt{\frac{4 \times A_B}{\pi}} \quad (1)$$

(b) Ellipsoidal bubble

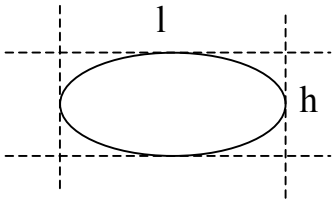

$$D_{Bm} = \sqrt[3]{(l^2 \times h)} \quad (2)$$

Figure 4. Typical bubble generation shape photographs

The bubble formation frequency f_B (i.e., the number of bubbles formed at the membrane orifice per unit time) is determined as Eq. (3) [5]:

$$f_B = \frac{Q_G}{V_B} \quad (3)$$

where V_B is the average detached bubble volume and Q_G is the gas flow rate measured using the soap film meter.

Thanks to the image treatment system, the terminal rising bubble velocities (U_B) can be estimated for the most frequent bubble diameter; two calculating methods are used to determine these velocities [17]:

- By measuring the distance between two frames:

$$U_B = \frac{\Delta D}{T_{frames}} \tag{4}$$

where ΔD is the bubble spatial displacement between t = 0 and t = T_{frames} = 1/120 s.

- By following the variation in the bubble extremity coordinates with time:

$$U_B = \frac{dy}{dt} \tag{5}$$

where y is the ordinate of the bubble center of gravity.

2.3 LIQUID PHASE CHARACTERISATION

To understand the effect of surfactants on the mass transfer efficiency, it is essential to well characterise the liquid phases under test: tap water and aqueous solutions with surfactants (cationic and anionic type); the surfactants have been chosen with regards to their nature and application (waste water treatment). Given that these liquids are dilute aqueous solutions, their density and viscosity are assumed to be equal to those of tap water (997 kg/m^3 and.10^{-5} Pa.s respectively). Thus, the liquid phase characterisation will consist in determining their static and dynamic surface tensions and some other properties, such as Critical Micelle Concentration (CMC) and adsorption parameters.

a. Static and dynamic surface tensions

The static surface tension measurements are performed by the Digidrop (GBX) and Krüss tensiometers based on the pendant drop method. Note that the static methods have a major drawback for modelling the bubble growth: the surface age is not taken into account. The static surface tension and the chemical properties of the liquid under test are reported in Table 2. The lowest surface tension is obtained for the cationic surfactant solution with 2000 mg/l and the highest for tap water. The dynamic surface tension obtained by Loubière and Hébrard [7] has to be considered to provide a better understanding of the adsorption and diffusion

kinetics of surfactant molecules up to the bubble surface. This study has shown that the diffusion kinetics obtained for the anionic surfactant solution are faster than those for the cationic solution, and that the time necessary to reach the surface tension at equilibrium decreases as the surfactant concentration increases.

b. Critical Micelle Concentration (CMC)

For the two surfactant type aqueous solutions, the static surface tension is determined for several concentrations. When the surfactant concentration increases, the surface tension tends to decrease until levelling off: the solution is then saturated in surfactants (formation of micelles), the Critical Micelle Concentration (CMC) is reached. Deduced from these curves, the CMC of each surfactant is reported in Table 2.

Table 2. Chemical characteristics of liquid phases

Solution Type	Chemical Name	$[C]^{(*)}$ (mg/l)	CMC (mg/l)	$M^{(**)}$ (kg/mol)	σ_L (mN/m)	Γ_∞ (mol/m^2)	K (m^3/mol)	S_e
Tap Water	-	-	-	18.10^{-3}	71.8	-	-	0
Anionic surfactant	Sodium laurylsulfate	1900	1900	$\cong 382.10^{-3}$	39,7	$3.52.10^{-5}$	6.25	1
		110	1900	$\cong 382.10^{-3}$	65	$3.52.10^{-5}$	6.25	0.6
Cationic surfactant	Lauryl dimethyl benzyl ammonium bromine	2000	920	$\cong 400.10^{-3}$	27.6	$3.49.10^{-5}$	90.9	1
		110	920	$\cong 400.10^{-3}$	42.4	$3.49.10^{-5}$	90.9	0.92

$^{(*)}$ [C] is the concentration used for experiments

$^{(**)}$ M is the molecular concentration

c. Characteristic adsorption parameters

To characterize the adsorption of solute molecules at a gas-liquid interface, Loubière and Hébrard [7] used the method based on the Langmuir theory. In this case, the kinetics of

adsorption and diffusion of the surfactant molecules towards the bubble interface can be described by the following equations [18]:

$$s_e = \frac{\Gamma_e}{\Gamma_\infty} = K\frac{C}{1+KC} \tag{6}$$

$$\sigma_{L,O} - \sigma_L \approx RT_a.\Gamma_\infty.Log\ \ (K) + RT_a.\Gamma_\infty.Log\ \ (C) \tag{7}$$

where s_e is the surface coverage ratio at equilibrium, C the solute concentration in the liquid phase, Γ_∞ the surface concentration when it is saturated, K the adsorption constant at equilibrium, $\sigma_{L,0}$ the surface tension when the solvent is pure and T_a the adsorption temperature.

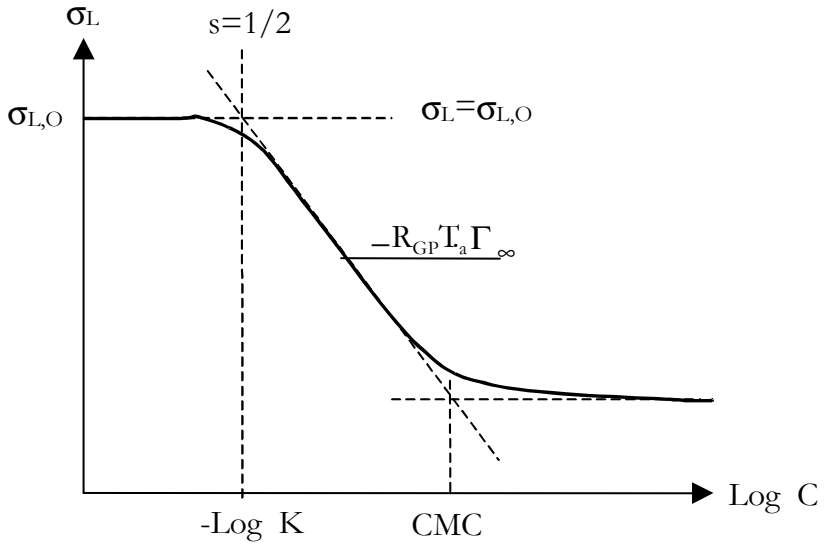

Figure .5 Diagram for determining the characteristic adsorption parameters (K and Γ_∞) by using the relations between surface tension and Log (C) (Eqs. (6-7))

The surface concentration at saturation Γ_∞ is determined by taking the slope of the curve relating σ_L to Log(C) before CMC is reached (Figure 5). Then, its intersection with the horizontal asymptote ($\sigma_L=\sigma_{L,0}$ when C tends to zero) allows the adsorption constant at the equilibrium K to be obtained (Log(K) = -Log(C)): at this point, the recovery rate s is equal to 0.5. From the values of C, K and Γ_∞, the surface coverage ratio s_e is deduced (Eq. (7)). The

characteristic adsorption parameters K, Γ_∞ and s_e are reported in Table 2. It can be noted that the surface concentrations at saturation Γ_∞ are quite similar whereas the adsorption constant at equilibrium K depends on the surfactant solutions. The K value of cationic surfactant is larger than that of the anionic: at the adsorption equilibrium, the cationic surfactant molecules have thus a higher affinity towards the bubble interface than the anionic molecules. The values of the surface coverage ratio s_e increase with the solute concentration C in the liquid phase (which is assumed to be 0 in the case of water). Furthermore, the surface coverage ratio s_e is equal to 1 when the concentration is higher than the CMC: the interface is thus saturated.

2.4 MASS TRANSFER PARAMETER DETERMINATION

In this present study, the local interfacial area provided by a single orifice sparger and the corresponding volumetric mass transfer coefficient are determined by a new local experimental approach, allowing the local liquid-side mass transfer coefficient to be calculated.

a. Local interfacial area (a)

Key parameter in the study of the gas-liquid mass transfer, the interfacial area can be determined by several methods: although the chemical methods are the most frequently used (for example the Danckwerts method based on the absorption of CO_2 in sodium or potassium carbonate-bicarbonate buffer solution [15]), the interfacial area can also be estimated by taking into account the bubble size and the gas hold-up [10, 19].

In this work, the local interfacial area is defined as the ratio between the bubble surfaces (S_B) and the total volume in reactor (V_{Total}). The number of bubbles (N_B) is deduced from the terminal rising bubble velocities (U_B) and the bubble formation frequency (f_B) as :

$$N_B = f_B \times \frac{H_L}{U_B} \tag{8}$$

The velocities U_B, determined as previously described (§ 2.2), have been validated by the experimental curves of Grace and Wairegi [20]. Consequently, the interfacial area is expressed as Eq. (9):

$$a = N_B \times \frac{S_B}{V_{Total}} = f_B \times \frac{H_L}{U_B} \times \frac{S_B}{A.H_L + N_B.V_B} \quad (9)$$

Depending on the bubble shape, the bubble surfaces are calculated,

- for spherical bubble, as: $S_B = \pi.D_B^2$ (10)
- for ellipsoidal bubble, as: $S_B = 2.\pi.[\frac{l^2}{4} + (\frac{l^2}{4} \times \frac{1}{2.e}.ln\frac{(1+e)}{(1-e)})]$ (11)

where e is the ratio between *h* and *l*, H_L and A the liquid height (H_L = 0.25 m) and the cross-sectional area (A = 0.0173 m^2) respectively. According to Eq. (9), the interfacial area is a function of the bubble formation frequency, the terminal bubble rising velocity and the generated bubble diameter.

b. Local volumetric mass transfer coefficient

Two methods are used to determine the local volumetric mass transfer coefficient:

Non-stationary or dynamic method (Classical method) [21]

This method consists in passing nitrogen through the liquid phase in order to remove the oxygen content and to replace it with air at the beginning of the experiment. The oxygen concentration in the liquid phase is measured with the UNISENSE oxygen microsensor which is a miniaturized Clark-type oxygen sensor with an internal reference and a guard cathode. This sensor is connected to a high-sensitivity picoammeter, allowing the resulting reduction current from the oxygen penetration at the gold cathode surface to be converted into a signal. The convertion of this signal into an equivalent concentration of oxygen (C_L) is performed by considering a linear conversion and by multiplying with the atmospheric level solubility.

During the experimental run , sufficient time is available to reach the oxygen saturation C_L* in the liquid. The response time of this UNISENSE probe is very fast (as low as 50 ms), it corresponds to the experimental error which has been estimated to ± 2 % for the k_La determination.

In the application of this method, the following assumptions are made: the response time of the probe is negligible, the liquid phase is perfectly mixed, the oxygen depletion from gas bubbles is negligible. As the oxygen concentration increases, the mass transfer rate is given by the following equation:

$$\frac{dC_L}{dt} = k_L a.(C_L^* - C_L) \tag{12}$$

or, in its integral form by:

$$ln(C_L^* - C_L) = ln(C_L^*) - k_L a.t \tag{13}$$

where C_L and C_L^* are the dissolved oxygen concentration and the saturation oxygen concentration in the liquid phase respectively. Thus, the local volumetric mass transfer coefficient k_La is deduced from the slope of the curve relating the variation of ln(C*-C) with t.

Mass balance on the quantity of sodium sulphite (New method)

This new k_La determination method is based on a mass balance on sodium sulphite (Na_2SO_3) concentration during the aeration time. Nitrogen is firstly injected into the liquid phase in order to eliminate the dissolved oxygen present in the bubble column. When the concentration of dissolved oxygen (O_2) reaches nearly zero, fresh oxygen, issued from air, is introduced and will react with the small quantity of Na_2SO_3: this step has been limited to 2 minutes. Note that an excessive use of Na_2SO_3 should be avoided as it would affect the coalescing properties of liquid phase. Thus, an adequate amount of Na_2SO_3 has to be found for keeping a zero O_2 concentration during the aeration step. This experimental process is shown in Figure 6.

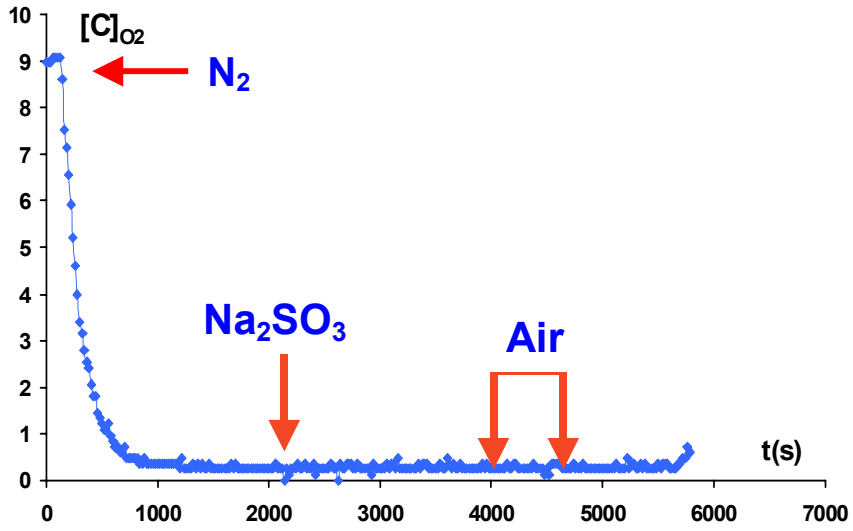

Figure 6. Experimental process related to the new k_La determination method

For a given hydrodynamic condition and for a given driving force for mass transfer, the enhancement factor (E) is defined as the ratio between the absorption flux in the presence of the third dispersed phase (Na_2SO_3) and in its absence [22]. In the present experiments, this factor has been estimated: it is close to 1. There is no deflection in the concentration gradient (no reaction) in the film at the interface and hence, mass transfer from the gas phase will occur totally in the liquid phase [23].

The chemical reaction between Na_2SO_3 and O_2 transferred can be expressed as:

$$Na_2SO_3 + \frac{1}{2}O_2 \longrightarrow Na_2SO_4$$

Subsequently, the total consumption of Na_2SO_3 can be deduced from a mass balance as the following equation shows:

$$m_T = m_S + m_R \qquad (14)$$

m_T is the total mass of Na_2SO_3 initially introduced (from 5 to 75 mg). It leads to Na_2SO_3 concentrations varying between 10 and 150 mg/L: adequate for the experimental process, these concentrations don't modify the bubble coalescence [24]. m_S is the mass of Na_2SO_3 reacting with the oxygen dissolved during the stationary regime and m_R is the mass of Na_2SO_3

remaining in the column and determined by an iodometry method [25]. According to this method, the determination of the Na_2SO_3 concentration is based on two measurement steps:

1. Determination of the initial quantity of iodine (I_2) formed by the reaction associated with the following solution: potassium iodate (**KIO_3**), potassium iodide (KI) and sulfuric acid (H_2SO_4);
2. Use of sodium thiosulfate ($Na_2S_2O_3$) to measure the remaining quantity of I_2 after reaction with Na_2SO_3.

Consequently, the quantity of I_2 consumed during the reaction with Na_2SO_3 can be determined and used to calculate the quantity of Na_2SO_3 remaining in the column (m_R). From the values of m_T and m_R, m_S is deduced. Thus, the quantity of transferred oxygen m_{O_2} is expressed as Eq. (15):

$$m_{O_2} = \frac{1}{2}\frac{M_{O_2}}{M_{Na_2SO_3}}.m_S = \frac{1}{2}\frac{M_{O_2}}{M_{Na_2SO_3}}.(m_T - m_R) \tag{15}$$

The molecular mass of O_2 and Na_2SO_3 (noted M_{O_2} and $M_{Na_2SO_3}$) are equal to 32 and 126 g/mol respectively. As the O_2 concentration remains zero throughout the experimental time, the oxygen transfer rate during the aeration time can be presented as Eq. (16):

$$\phi = \frac{m_{O_2}}{t_{Aeration}} = k_L a.V_L.C^* \tag{16}$$

where $t_{Aeration}$ is the aeration time (2 minutes), C* and V_L the saturation oxygen concentration in the liquid phase and the volume of liquid in the reactor respectively. Consequently, the local volumetric mass transfer coefficient can be expressed as Eq. (17):

$$k_L a = \frac{\frac{1}{2}\frac{M_{O_2}}{M_{Na_2SO_3}}.(m_T - m_R)}{t_{Aeration}.V_L.C^*} \tag{17}$$

c. Liquid-side mass transfer coefficient (k_L)

The liquid-side mass transfer coefficient represents an essential part for the enhancement factor calculations in the case of instantaneous and fast reactions. Commonly reported as a function of liquid properties and bubble size [21], it depends also on the diffusivity coefficient and on the flow pattern around the bubbles (local hydrodynamics). Several empirical and/or theoretical correlations for determining k_L in various systems are summarized in [21, 23, 26]. Note that the chemical method (based on the Danckwerts method) is the most frequently used to estimate the liquid-side mass transfer coefficient [14-15, 27].

The product of the liquid-side mass transfer coefficient (k_L) and the interfacial area (a) is known as the volumetric mass transfer coefficient (k_La). Thus, the local liquid-side mass transfer coefficient can be simply determined by Eq. (18):

$$k_L = \frac{k_L a}{a} \tag{18}$$

3. RESULTS AND DISCUSSION

3.1 EFFECT OF SURFACTANTS ON THE BUBBLES GENERATED

a. Bubble diameter (D_B)

Figure 7 shows the relation between the detached bubble diameter and the gas flow rate for the different liquid phases, each liquid phase being characterized by the surface coverage ratio (s_e) reported in Table 2. Firstly, this figure highlights the logarithmic increase in bubble diameter with gas flow rate typically observed with membrane spargers [5]. At low gas flow rates (Q_G < 1 ml/s), the bubble diameters obtained with cationic and anionic surfactant solutions are lower than those obtained with tap water. As proposed by Loubière and Hébrard [7], these results should be due to the differences observed in terms of dynamic surface tensions, and to their consequences on the balance between the surface tension and the

buoyancy forces during the bubble growth and detachment. At high gas flow rates, the differences in terms of bubble diameters are directly linked to static surface tension values. In fact, in this range of gas flow rates, the bubble diameter is no more controlled by the force balance at detachment, but rather by the power dissipated in the liquid, conditioning the bubble break up and coalescence phenomena.

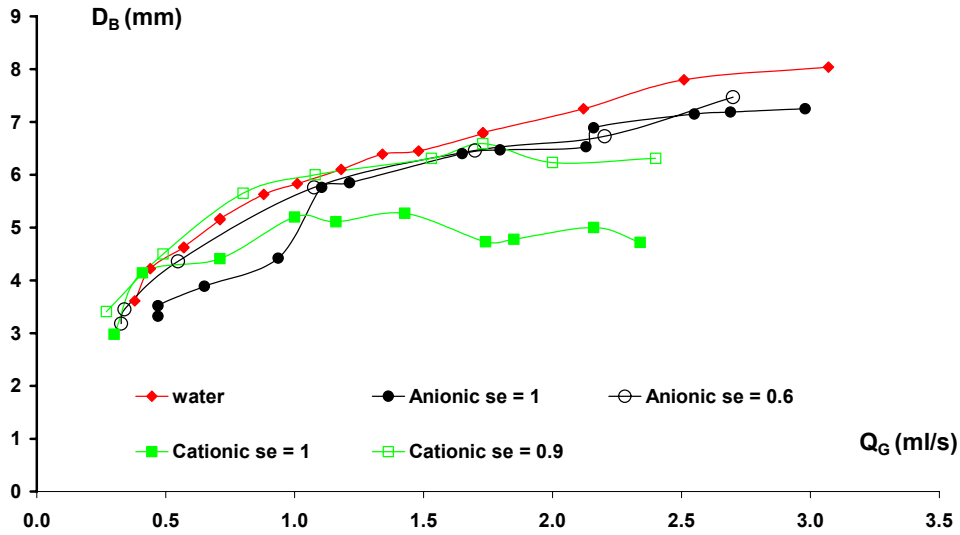

Figure 7. Bubble diameter versus gas flow rate

For a given gas flow rate and a given surfactant solution, the D_B values associated with the surface coverage ratio at equilibrium s_e equal to 1 are smaller than those obtained from the low s_e values (0.6 and 0.9 for the anionic and cationic surfactants respectively). This clearly proves that a modification of surfactant concentration (i.e, of surface tension value and of surface coverage ratio at equilibrium) affects the generated bubble diameters.

b. Bubble formation frequency (f_B)

The relation between the bubble formation frequency (Eq. (3)) and the gas flow rate is shown in Figure 8 for the different liquid phases.

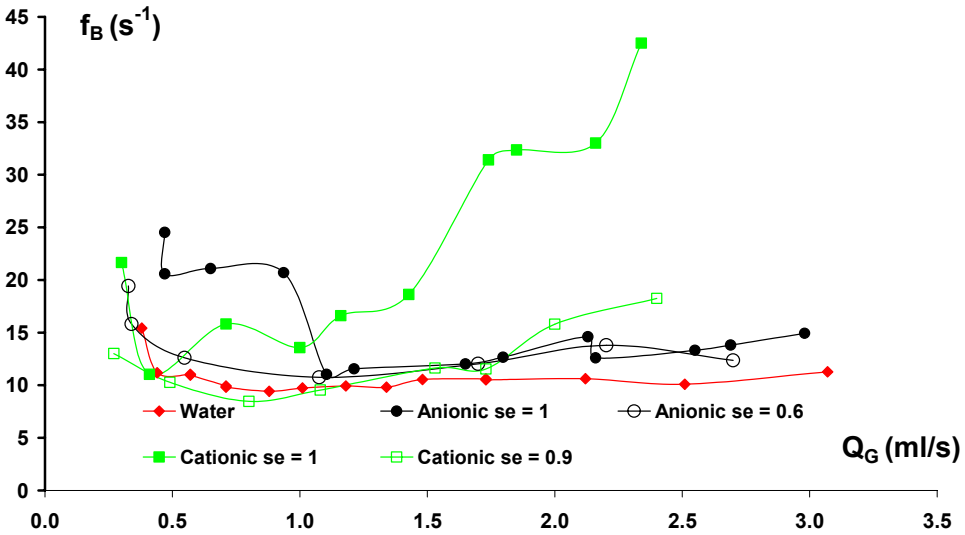

Figure 8. Bubble formation frequency versus gas flow rate

The bubble formation frequencies obtained with surfactants are on average larger than those with water, except for low gas flow rates where the smallest frequencies are observed for cationic surfactants. In the case of water and anionic surfactant solutions, the bubble formation frequency reaches a constant value (about 10-15 s^{-1}) above critical gas flow rates whereas it increases continuously for cationic surfactants.

c. Terminal rising bubble velocitiy (U_B)

Figure 9 shows, for the different liquid phases, the relation between the terminal rising bubble velocity and the bubble diameter generated.

Over the whole bubble diameter range (3-8 mm), the terminal rising bubble velocities (obtained experimentally) vary between 18 and 24 cm/s and are closed to those given by Grace and Wairegi [20]. These results shows also that the terminal rising bubble velocity is affected by some modifications of surfactant concentrations

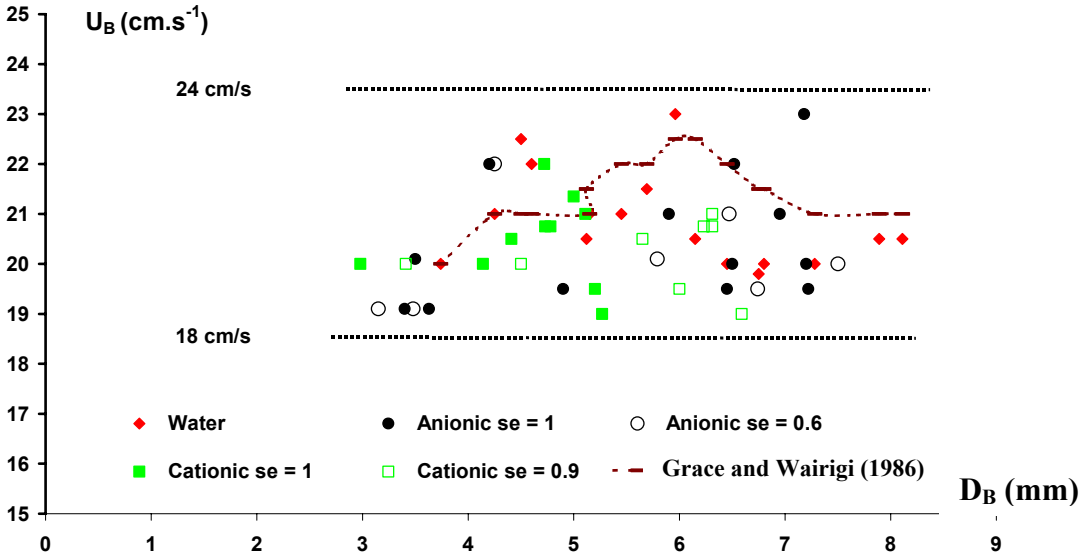

Figure 9. Terminal rising bubble velocity versus bubble diameter

d. Interfacial area (a)

The variations of the interfacial area (Eq. (9)) with the gas flow rate are plotted in Figure 10 for the different liquid phases.

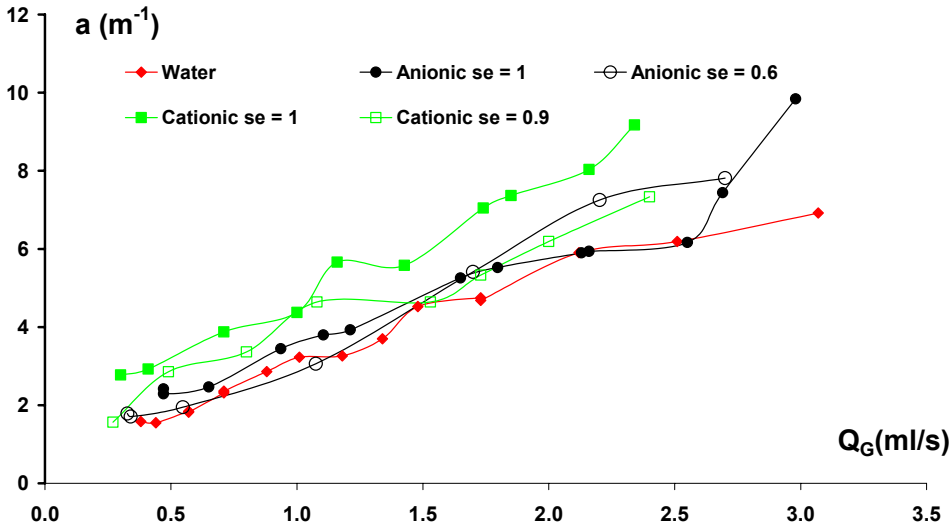

Figure 10. Interfacial area versus gas flow rate

Whatever the liquid phases, the interfacial area increases roughly linearly with the gas flow rate. Their values vary between 1.5 and 10 m^{-1} for gas flow rates varying between 0.3 and 3.5 ml/s. The interfacial areas related to surfactant solutions are significantly larger than those of

water. For a given gas flow rate and a given surfactant solution, the values of a obtained with s_e equal to 1 are larger than those obtained with lower s_e values; these results are directly correlated with those of D_B, f_B and U_B (Figures 7-9).

The effects of surfactants on the bubble formation phenomenon and on the interfacial area being clearly proved, their consequences on the mass transfer parameters have to be evaluated now: this is the aim of the next section.

3.2 EFFECT OF SURFACTANTS ON THE MASS TRANSFER PARAMETERS

a. Local volumetric mass transfer coefficient (k_La)

In Figure 11, the volumetric mass transfer coefficients (k_La) obtained with the new method are compared with those of the classical method (§ 2.4.b).

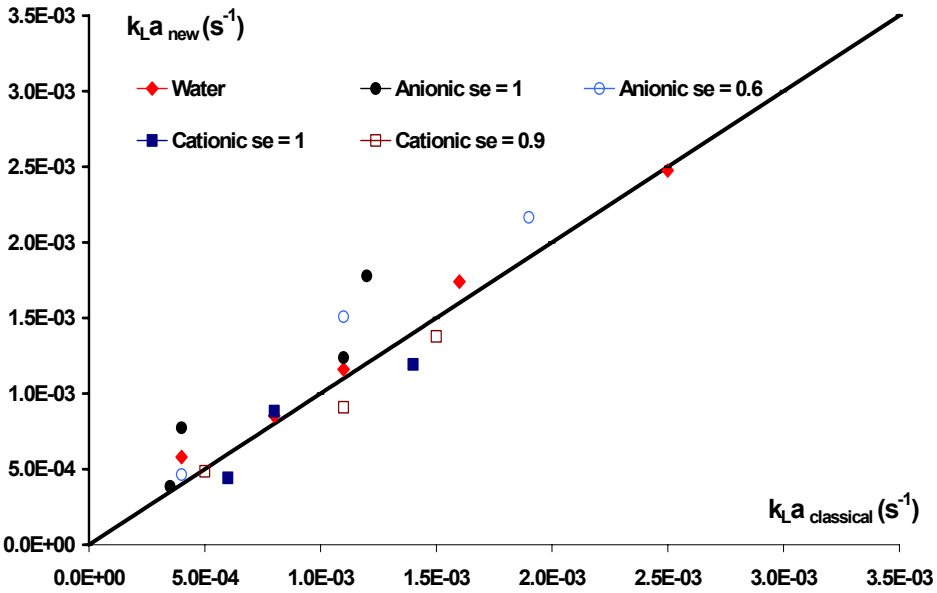

Figure 11. Comparison of the two methods for calculating the volumetric mass transfer coefficients

Except for some cases relating to the anionic surfactant, the average differences between the two methods are about ± 15 %, which corresponds to the experimental error associated with the new method. Note that the advantage of the developed method is that it is not required to consider the mixing in the liquid phase.

Figure 12 presents the variation of the volumetric mass transfer coefficient (k_La) with the gas flow rate for the different liquid phases.

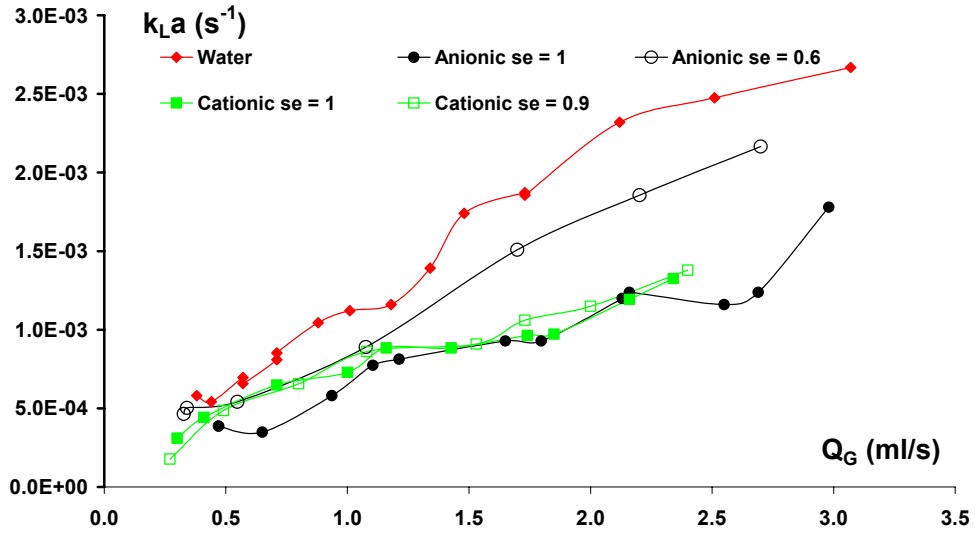

Figure 12: Volumetric mass transfer coefficient versus gas flow rate

This last figure indicates that, whatever the liquid phases, the volumetric mass transfer coefficient increases with the gas flow rate. The values of k_La vary between 0.00035 and 0.003 s^{-1} for gas flow rates varying between 0.3 and 3.5 ml/s. The volumetric mass transfer coefficients of both surfactant solutions are significantly smaller than those of water. For a given gas flow rate and a given surfactant solution, the lowest k_La values are obtained with the surface coverage ratio at equilibrium equal to 1; this means that the presence of surfactants, even in small quantities, can have significant effects on the mass transfer mechanism.

To well understand these phenomena, the liquid-side mass transfer coefficient (k_L) has to be considered separately.

b. Local liquid-side mass transfer coefficient (k_L)

Figure 13 shows the variation of the liquid-side mass transfer coefficient (k_L) with the gas flow rate for the different liquid phases. The values of k_L exhibit a degree of scattering, this is due to the fact that the calculation of k_L (Eq. (18)) accumulates the experimental errors associated with measurements of both k_La and a. The average and maximum experimental error for determining the k_L value have been estimated at ± 10% and ± 15% respectively.

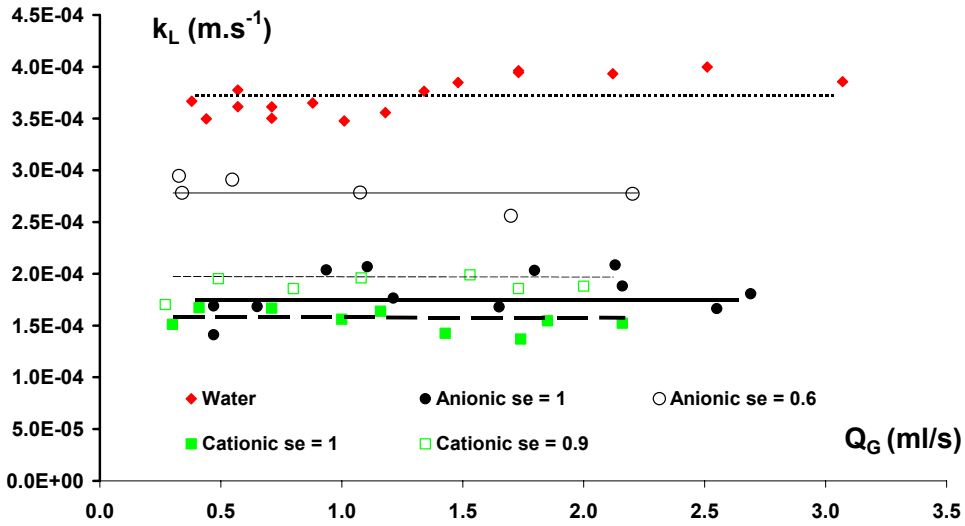

Figure 13. Liquid-side mass transfer coefficient versus gas flow rate

According to Figure 13, the values of k_L obtained vary between 0.00010 and 0.00045 $m.s^{-1}$ for gas flow rates varying between 0.3 and 3.5 ml/s. Whatever the gas flow rates, the k_L values remain roughly constant for each liquid phase. The k_L values of both surfactant solutions are significantly smaller than those of water: these results clearly indicate that the presence of surfactants at the bubble interface disturbs the mass transfer, certainly by modifying the composition or the thickness of liquid film around the air bubbles.

For a given gas flow rate and a given surfactant solution, the k_L values obtained with the surface coverage ratio at equilibrium equal to 1 are smaller than those for the other lower s_e. Moreover, the k_L values related to high surfactant concentrations (i.e. $s_e = 1$) are quite similar, whereas significant differences appear in the case of low surfactant concentrations (120 mg/l).

At this stage, it can be assumed that the increase in s_e should decrease the gas diffusivity and thus modify the resistance of the gas-liquid interface. As a result, the decreasing mass transfer coefficients (k_La and k_L) in the presence of surfactants would be the consequence of a modification of the gas-liquid interface nature coupled with local hydrodynamic changes [22]. The negligible differences between k_L values when s_e equals 1 should be due to the close surfactant molecule sizes (382 g/mol and 400 g/mol for anionic and cationic surfactant respectively).

Figure 14 presents the variation of the liquid-side mass transfer coefficient (k_L) with the bubble diameter generated (D_B) for the different liquid phases.

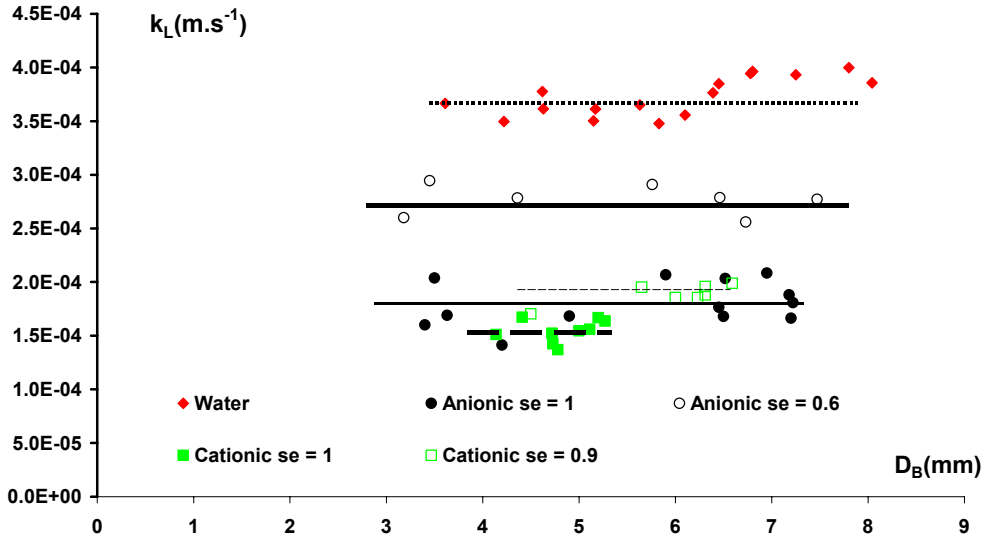

Figure 14. Liquid-side mass transfer coefficient versus bubble diameter

According to Figure 14, the k_L values vary between 0.00015 and 0.00045 $m.s^{-1}$ for bubble sizes varying between 3 and 8 mm. The k_L values for both surfactant solutions (anionic and cationic) do not depend on the bubble diameter. These results agree with those of Calderbank and Moo-yong (1961): the authors have shown that the k_L values are constant for bubbles having diameters greater than 3 mm behaving usually like fluid particles with a mobile surface.

All these results have pointed out the existence of a direct relationship between the surface coverage ratio (s_e) and the mass transfer coefficient (k_La and k_L), as well as the fact that physical-chemical properties (liquid surface tension, surface coverage ratio at equilibrium) in the case of concentrated liquid phase are the important parameters to consider in the study of mass transfer.

3.3 MODEL FOR DETERMINING THE LIQUID SIDE MASS TRANSFER COEFFICIENT

a. Comparison with existing models

The literature [13, 28] related to k_L shows that the experimental k_L values vary between the two equations:

- Higbie [26]: $$k_L = 2\sqrt{\frac{D_{O2}.U_B}{\pi.h}} \quad (19)$$

- Frossling [26]: $$k_L = \frac{D}{D_B}(2 + 0.6.Re^{\frac{1}{2}}.Sc^{\frac{1}{3}}) \quad (20)$$

where h is the bubble height, close to its diameter at low gas flow rates(Figure 4),. Re the bubble Reynolds number and Sc the Schmidt number.

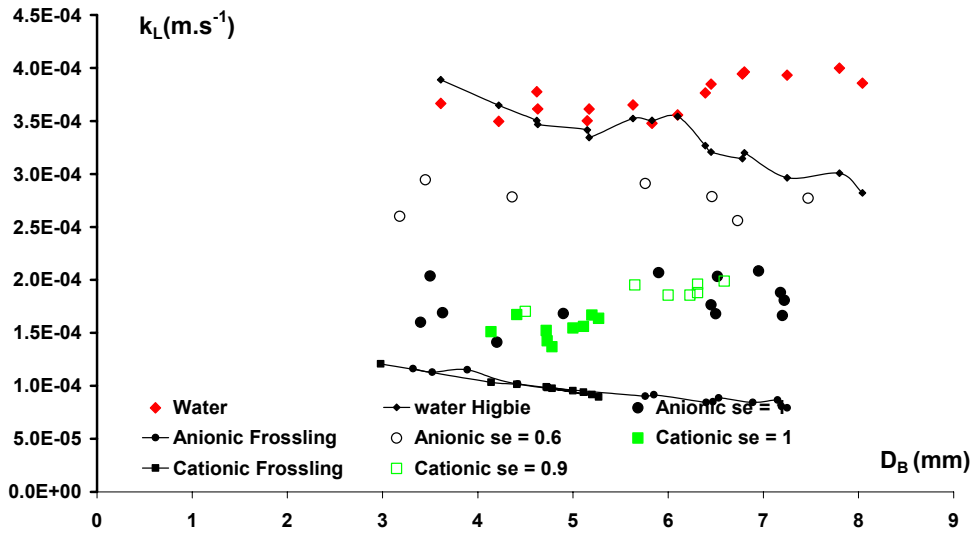

Figure 15. Comparison of liquid-side mass transfer coefficient with the existing models

The Higbie's theory [27] is valid for mobile spherical bubbles ($D_B > 2.5$ mm) having short contact times with the liquid, whereas the Frossling's equation deals with spherical bubbles having rigid interface (0.1 mm < D_B < 2 mm).

A comparison between these two models and the present experimental results is shown in Figure 15. The following comments can be made:

- the k_L values obtained with Higbie's equation are close to those obtained with tap water ($s_e = 0$) at low bubble diameters ($D_B < 6$ mm), but significant differences appear at larger D_B. The ellipsoid bubble shape is probably responsible for these results;
- the k_L values related to $s_e = 1$ for both surfactants are quite similar to those deduced from the Frossling equation at small bubble diameters, but they diverge at larger D_B;
- if there is just a small amount of surfactants in the liquid phase (0 < se < 1), both equations (Higbie and Frossling) are not adequate to predict the intermediate k_L values. These results agree with Hébrard et al. [29] and Vasconcelos et al. [13].

To determine the intermediate k_L values in the presence of surfactants, Vasconcelos et al. [13] have proposed a model where the contamination kinetics of a single bubble, is considered and coupled with a sudden surface transition from a mobile to a rigid condition, in agreement with the stagnant cap model. In the present operating conditions, the changes in the bubble diameter (from mobile to rigid condition) with time does not occur, implying that the model proposed by Vasconcelos et al. [13] cannot be applied. In fact, Loubière and Hébrard [7] have shown that the effect of surfactants on the bubble diameter was instantaneous because of linked to fast kinetics of adsorption and diffusion of surfactant molecules towards the bubble interface.

Thus, the gap of existing models consists mainly not in taking sufficiently into account the dynamic properties of surfactants.

b. Prediction of k_L based on the surface coverage ratio

With regard to its importance, the surface coverage ratio (s_e) is chosen to classify the bubbles according to their interface "nature": $s_e = 0$ corresponds to a free interface (water in this work), $s_e = 1$ to a saturated interface and $0 < se < 1$ to a non-saturated interface.

The average k_L values are assumed to vary between the two k_L limits (noted k_L^0 and k_L^1) associated with $s_e = 0$ and $s_e = 1$ respectively. In order to predict k_L in the presence of surfactants, the following relation is proposed:

$$k_L = k_L^1 . s_e + k_L^0 . (1 - s_e) \qquad (21)$$

where k_L is the liquid-side mass transfer coefficient independent of the operating conditions (Figure 14).

Figure 16 presents the variations of the experimental and predicted liquid-side mass transfer coefficients (k_L) with the bubble diameter generated (D_B) for the different liquid phases

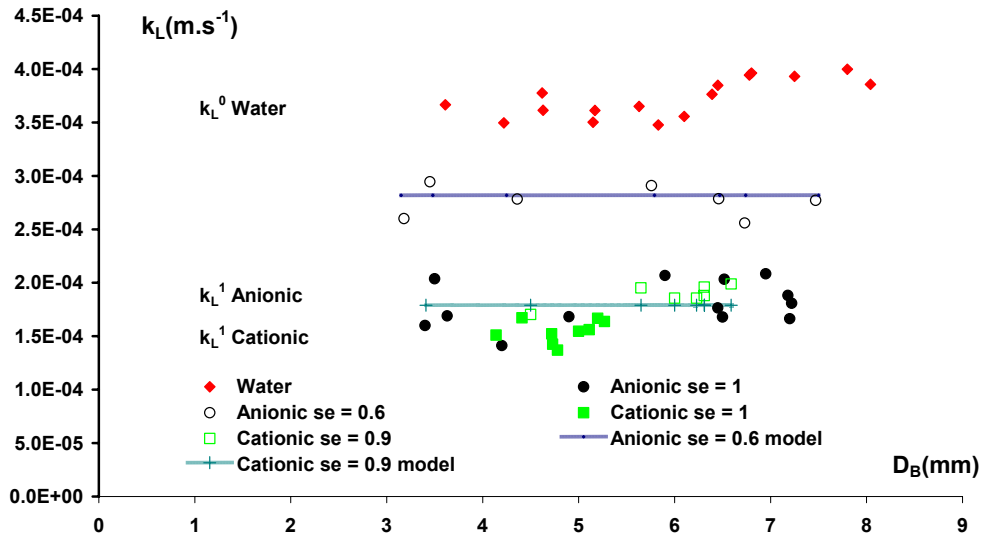

Figure 16. Comparison of experimental and predicted liquid-side mass transfer coefficients

This figure shows that a quite good agreement between the experimental and the predicted k_L is obtained (average difference about $\pm 10\%$). However, more experimental data are necessary to validate this model more accurately: in the future, other surfactants and gas spargers will be tested to extend the operating condition ranges. Furthermore, the gas diffusivity D in the presence of surfactant solutions and in conditions where the hydrodynamic is perfectly controlled will be carefully studied to improve the modeling and hence to provide a better understanding of the gas-liquid mass transfer mechanisms.

4. CONCLUSION

This study has shown that the presence of surfactants affects the bubble generation process, hence the interfacial area (a) and the different mass transfer parameters such as the volumetric mass transfer coefficient (k_La) and the liquid-side mass transfer coefficient (k_L). The new k_La determination method has provided good accuracy whatever the operating conditions, without needing to assume that the liquid phase is perfectly mixed as in classical method. Furthermore, the following results have been obtained:

- The volumetric mass transfer coefficient increases with the gas flow rates whatever the liquid phases and the k_La values for both surfactants are significantly smaller than those of water;
- Whatever the bubble diameters, the liquid-side mass transfer coefficient remains roughly constant for a given liquid phase;
- The k_L values for both surfactants are significantly smaller than those of the water;
- If there is only a small amount of surfactants in the liquid phase ($0 < se < 1$), the equations deduced from the Higbie's and Frossling's theories cannot be applied to predict the k_L;

- The physico-chemical properties such as liquid surface tension and surface coverage ratio (s_e) prove to be the important parameters to consider for predicting the variation of the k_L values.
- The simple model proposed, based on the use of the surface coverage ratio, has allowed a quite good agreement between the experimental and predicted k_L. to be obtained (average difference about ± 10%).

In the future, it will be essential to study carefully the gas diffusivity D in the presence of surfactants and in conditions where the hydrodynamic is perfectly controlled: this will be one of the key for modeling the k_L^1 value for each type of surfactant and hydrodynamic condition. Moreover, is evident that the results observed in our little bubble column volume have to be validated into a tall bubble columns and at higher superficial velocities.

ACKNOWLEDGEMENTS

The authors gratefully acknowledge Bernard REBOUL for his technical support.

NOTATION

A	cross-sectional area of reactor	$[m^2]$
A_B	bubble area	$[m^2]$
a	interfacial area	$[m^{-1}]$
C_L	dissolved oxygen concentration	$[kg/m^3]$
C_L*	oxygen concentration at saturation	$[kg/m^3]$
C	solute concentration in liquid phase	$[kg/m^3]$
CMC	Critical Micelle Concentration	$[kg/m^3]$

D	gas diffusivity	$[m^2/s]$
D_B	bubble diameter	[m]
D_{OR}	equivalent hole diameter	[m]
E	enhancement factor	[-]
f_B	bubble formation frequency	$[s^{-1}]$
H_L	liquid height	[m]
K	adsorption constant at the equilibrium	$[m^3/mol]$
k_L	liquid-side mass transfer coefficient	[m/s]
k_La	volumetric mass transfer coefficient	$[s^{-1}]$
M	molecular mass	[kg/mol]
m_R	mass of Na_2SO_3 remaining in the column	[kg]
m_S	mass of Na_2SO_3 reacting with the dissolved oxygen	[kg]
m_T	total mass of Na_2SO_3 introduced initially	[kg]
N_B	number of bubbles generated	[-]
Q_G	gas flow rate	$[m^3/s]$
S_B	total bubble surface	$[m^2]$
s_e	surface coverage ratio at equilibrium	[-]
$t_{Aeration}$	aeration time	[s]
T	temperature	[°C]
U_B	bubble rising velocity	[m/s]
U_G	gas velocity through the orifice	[m/s]

V_C	gas chamber volume between the control valve and the orifice		[m^3]
V_B	bubble volume		[m^3]
V_L	liquid volume in reactor		[m^3]
V_{Total}	total volume in reactor		[m^3]

Dimensionless numbers

Sc	Schmidt number defined by	$Sc = \frac{\mu_L}{\rho_L . D}$	[-]
Re	Bubble Reynolds number defined by	$Re = U_B . \rho_L . D_B / \mu_L$	[-]
Re_{OR}	Hole Reynolds number defined by	$Re = U_G . \rho_G . D_{OR} / \mu_G$	[-]
We	Weber number defined by	$We = U_G^2 . d_{OR} . \rho_G / \sigma_L$	[-]

Greek symbols

γ_C	wetting critical surface tension of the membrane surface	[N/m]
μ_L	liquid viscosity	[Pa.s]
ρ_L	liquid density	[kg/m^3]
σ_L	liquid surface tension	[N/m]
$\sigma_{L,0}$	surface tension when the solvent is pure	[N/m]
Γ_∞	surface concentration when it is saturated	[mol/m^2]

REFERENCES

[1] Rice R.G., Tupperainen J.M.I, Hedge R., Dispersion and hold up in bubble columns. Comparison of rigid and flexible sparger, Canadian Journal of Chemical Engineering,

59 (1981) 677-687.

[2] Loubière K., Hébrard G., Bubble formation from a flexible hole submerged in an inviscid liquid, Chemical Engineering Science, 58 (2003) 135-148.

[3] Hébrard G., Bastoul D., Roustan M., Influence of the gas spargers on the hydrodynamic behaviour of bubble columns, Trans IchemE, 74 (A) (1996) 406-414.

[4] Couvert A., Roustan M., Chatellier P., Two-phase hydrodynamic study for a rectangular air-lift loop reactor with an internal baffle, Chemical Engineering Science, 54 (21) (1999) 5245-5252.

[5] Painmanakul P., Loubière K., Hébrard G., Buffière P., Study of different membrane spargers used in waste water treatment: characterisation and performance, Chemical Engineering and Processing, (2004) 1347-1359

[6] Li H.-Z., Du simple vers le complexe: une nouvelle approche des fluides non newtoniens, Habilitation à diriger des recherches, Institut National Polytechnique de Lorraine (1998).

[7] Loubière K., Hébrard G., Influence of liquid surface tension (surfactants) on bubble formation at rigid and flexible orifices, Chemical Engineering and Processing, (2004) 1361-1369

[8] Vázquez G., Cancela M. A., Varela R., Alvarez E., Navaza J. M., Influence of surfactants on absorption of CO_2 in a stirred tank with and without bubbling, Chemical Engineering Journal, 67 (1997) 131-137

[9] Akosman C., Orhan R., Dursun G., Effects of liquid property on gas holdup and mass transfer in co-current downflow contacting column, Chemical Engineering and Processing, 43 (2004), 503-509

[10] Bouaifi M., Hébrard G., Bastoul D., Roustan M., A comparative study of gas hold-up, bubble size, interfacial area and mass transfer coefficients in stirred gas-liquid reactors and bubble columns, Chemical Engineering and Processing , 40 (2001) 97-111.

[11] Zhao B., Wang J., Yang W., Jin Y., Gas–liquid mass transfer in slurry bubble systems: I. Mathematical modeling based on a single bubble mechanism, Chemical Engineering Journal, 96 (2003) 23-27.

[12] Zhao B., Wang J., Yang W., Jin Y., Gas–liquid mass transfer in slurry bubble systems: II. Mathematical modeling based on a single bubble mechanism, Chemical Engineering Journal, 96 (2003) 29-35.

[13] Vasconcelos J. M. T., Rodrigues J. M. L., Orvalho S. C. P., Alves S. S., Mendes R. L., Reis A., Effect of contaminants on mass transfer coefficients in bubble column and airlift contactors, Chemical Engineering Science, (2003) 1431-1440

[14] Vázquez G., Cancela M. A., Riverol C., Alvarez E., Navaza J. M., Application of the Danckwerts method in a bubble column: Effects of surfactants on mass transfer coefficient and interfacial area, Chemical Engineering Journal, 78 (2000) 13-19

[15] Cents A. H. G., Brilman D. W. F. and Versteeg G. F., Gas absorption in an agitated gas–liquid–liquid system, Chemical Engineering Science, 56 (2001) 1075-1083

[16] Castaignede V., Étude expérimentale et modélisation de la formation de bulles générées par un orifice flexible (membrane élastique) - Influence d'un courant liquide transversal, DEA, INSA, Toulouse (2001).

[17] Painmanakul P., Albespy S., Bonnet S., Marie C., Loubière K., Hébrard G., Mietton-Peuchot M., Bubble generation with a ceramic gas sparger classically used in the wine micro-oxygnation, Proceedings du 9ème congrès de la Société Française de Génie des Procédés (2003).

[18] Tauzin C., Contribution à l'étude et à la recherche d'applications spécifiques de la technique de fractionnement par bulles, Thesis dissertation No 23 INSA Toulouse, France (1979).

[19] Wongsuchoto P., Charinpanitkul T.and Pavasant P., Bubble size distribution and gas–liquid mass transfer in airlift contactors**,** Chemical Engineering Journal*,* 92 (2003) 81-90.

[20] Grace J.R., Wairegi T., Properties and Characteristics of drops and bubbles, Encyclopedia of Fluid Mechanics, Cheremisinoff. Chap 3, gulf Publishing Corporation, Huston, TX., (1986) 43-57.

[21] Deckwer W. D., Bubble column reactors, John Wiley & son Ltd, Baffins Lane, Chichester, England (1992)

[22] Dumont E., Delmas H., Mass transfer enhancement of gas absorption in oil-in-water systems: a review , Chemical Engineering and Processing, (2003) 419-438

[23] Roustan M., Transferts Gaz-Liquide dans les procédés de traitement des eaux et des effluents gazeux, TEC&DOC (2003).

[24] Lessard R. D., Zieminski S. A., Bubble coalescence and gas transfer in aqueous electrolytic solutions. Industrial and Engineering Chemistry, Fundamentals, 10, (1971) 260-289

[25] Pelizzari C., Etude du transfert d'oxygène dans un réacteur triphasique à lit fixe à cocourant ascendant d'eau et d'air, DEA, INSA, Toulouse, France (1995).

[26] Treybal R. E., Mass Transfer Operations, McGraw-Hill, New York (1980).

[27] Kulkarni A. A., Joshi J. B., Simultaneous measurement of flow pattern and mass transfer coefficient in bubble columns, Chemical Engineering Science, 59 (2004) 271-281

[28] Motarjemi M., Jameson G. J., Mass transfer from very small bubble – the optimum bubble size for aeration, Chemical Engineering Science, (1978) 1415-1423

[29] Hebrard G., Destrac P., Roustan M., Huyard A., Audic J. M., Determination of the water quality correction factor α using a tracer gas method, Water Research, (2000) 684-689